Activation and Cleavage of H−R Bonds through Intermolecular H···H Bonding upon Reaction of Proton Donors HR with 18-Electron Transition Metal Hydrides

Galina Orlova

Institute of Physical and Organic Chemistry, Rostov University, Rostov on Don, Russian Federation, 344090

Steve Scheiner* and Tapas Kar

Department of Chemistry, Southern Illinois University, Carbondale, Illinois 62901

Received: June 25, 1998

The H−R cleavage upon reaction MH + HR → MH···HR → M(η^2-H_2)R, where MH represents 18-e trans-dihydrides Ru(H)(H)($PH_2CH_2PH_2$)$_2$ (**1**), Ru(H)(H)(PH_3)$_4$ (**2**), Ru(H)(H)(NH_3)$_4$ (**3**); HR are HX (X = F, Cl) and HOR (R = H, CH_3) is studied using the DFT B3PW91/LANL2DZ level of theoretical calculations. The H−R bond splits upon interaction of the HR with **1** and **3** which possess a hydride H of high proton attracting power and significantly electropositive H of PH_2 and NH_3 groups. The basicity of the transition metal plays only a minor role in H−R splitting. The H−R cleavage proceeds via transfer of the H atom from R to hydride H in Ru−H···H−R···H−P(N), as an exothermic process without barrier or H···H intermediate. The less acidic HOR yields a multi-H-bonded intermediate Ru−H···H−O···(H−P(N))$_2$, where the H−O bond cleaves with a low barrier. Such an energetically facile mechanism of H−R splitting was not found for **2**, where H of PH_3 is too inert to interact with R and a multi-H-bonded complex is not formed. The computed relative energies and barriers are in agreement with available experimental data.

Introduction

The interaction between transition metal hydrides (MH) and proton donors (HR) appears to be one of the most important reactions in the chemistry of MH.[1−3] A new class of molecular η^2-H_2 complexes[2−7] has been obtained upon reaction 1

$$MH + HR \rightarrow M(\eta^2\text{-}H_2)^+R^- + M(H)_2^+ R^- \qquad (1)$$

where HR are strong proton donors such as HBF_4, Et_2O, or HPF_6. In the general case, this reaction affords a mixture of the η^2-H_2 molecular complex and classic trans-dihydride; both species are identified as ion pairs. The dynamic equilibrium between two salts has been experimentally and theoretically studied.[4−6]

Another class of compounds has been obtained recently upon reaction of MH with poorer proton donors in nonpolar media. It has been shown[3,8−10] that some MH involved in interaction with acid alcohols HOR yield intermolecular MH···HOR complexes of moderate stability. Some of these H···H complexes may undergo the following transformation to the η^2-H_2 species.

$$MH + HOR \rightarrow MH\cdots HOR \rightarrow M(\eta^2\text{-}H_2)OR \qquad (2)$$

Thus, ^{1}H NMR intermolecular dynamic equilibrium between H···H and η^2-H_2 complexes was supposed in the system (PH_2-CH_2PH_2)$_2$(H)RuH···H−OR ↔ ($PH_2CH_2PH_2$)$_2$(H)Ru(η^2-H_2)$^+$OR$^-$ (HOR is phenol or hexafluoroisopropyl).[11] The equilibrium at low temperature (240−230 K) suggested a low interconversion barrier. The high-barrier transformation from the H···H to the η^2-H_2 complex has been observed by IR and NMR spectroscopy for the intermolecular complexes of half-sandwich (Cp)Ru(CO)-(NO)H and (Cp)Re(PH_3)(NO)(H) with acid alcohols.[12] In both experiments, a proton transfer mechanism was suggested for (2), although the authors could not identify the system as unambiguously neutral or ionic**.**

Reaction 2 plays an important role in such processes as base-promoted heterolytic splitting of dihydrogen, formation of molecular η^2-H_2 complexes, and homogeneous catalysis by MH. In recent papers, we studied the peculiarities of the intermolecular H···H complexes[13] and model reaction 2 for the cationic system MH···H_3O^+ → M(η^2-H_2)H_2O^+.[14] It was suggested that the barrier of (2) in the case of neutral systems (which were studied in experiments[11,12]) depends mainly upon the energy of H−R bond cleavage. Nevertheless, the mechanism of (2) requires clarification, as does the reason for the wide range of reaction barriers that have been observed.

We attempt in the present paper to examine the likely mechanisms and suitable conditions of H−R splitting in noncharged systems as a key stage of pathway 2. Of particular interest here is the ability of the stable 18-e transition metal complexes to promote the cleavage of rather inert covalent bonds, an important matter in homogeneous transition metal catalysis.

Methods of Calculation

All calculations were carried out at the DFT level of theory with Becke's nonlocal exchange correction[16a] and Perdew and Wang's[16b] nonlocal correlation correction (B3PW91), using the Gaussian 94 package.[17] The standard LANL2DZ basis set[18] with effective core potential[19] was used. It has been shown that nonlocal (NL) corrections improve the computed results considerably.[20] In general, DFT NL correctly reflects most trends for transition metal complexes. Comparative analysis of the BLYP,[21a,21b] B3LYP,[16a,21b] and B3PW91 results shows that qualitatively similar conclusions are reached.[13,14,22] However, as has been shown in our earlier works[13,14] for the case of

10.1021/jp9827779 CCC: $18.00
Published on Web 01/13/1999

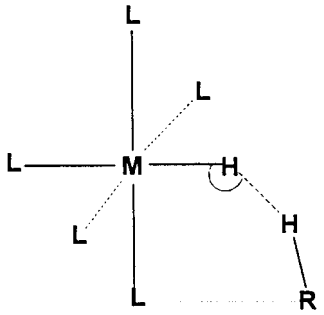

Figure 1. Generalized structure of intermolecular complex between HR and hexacoordinated MH. L represent ligands.

intermolecular H-bonded transition metal complexes, the B3PW91 geometries and bond energies are in overall best agreement with experimental data. Perdew's nonlocal correlation was used successfully by Ziegler's group for extensive investigations of Ziegler−Natta-type catalysts where H-bonding is involved.[23]

Potential energy profiles for H−R splitting were calculated by specifying the H−R distance as the reaction coordinate, while optimizing all other degrees of freedom. Hence, the minima and transition states reported below represent minima and maxima along these reaction profiles. Due to the inordinate expense of calculating second derivatives or examining a wide swath of the potential energy surface (PES) for these large systems, it was not feasible to search the entire surface for true minima, or to carry out full geometry optimizations in general. The nature of these structures as true minima, as well as the computation of vibrational frequencies, was reserved for geometries of particular importance.

Interaction energies of all types of complexes were computed as the difference between the total energy of the complex and the sum of the energies of the individual isolated subunits. Basis set superposition error was not corrected.

All the results pertain directly to the gas phase. Since reaction 2 appears to proceed even in nonpolar solvents it may be possible to exclude the influence of media on R−H cleavage for purposes of simplification.

General Preconditions for H−R Cleavage

An analysis of geometries of the H···H bonding complexes computed in previous works[13,14] reveals that preconditions for H−R splitting involve the structure of the intermolecular H···H complex itself, as depicted schematically in Figure 1. A principal feature of H···H bonding is the lengthening of the H−R bond, compared to a conventional H bond. The amount of this stretch is variable and depends mainly upon the strength of the H···H interaction and the acidity of HR. Another factor that may cause H−R lengthening is a weak interaction of R with coligands.

The computed[13,14] H−R stretches ΔR_{H-R} and the H···H bond lengths $R_{H...H}$ in some MH···HR complexes are listed in Table 1. The H−F bond lengthening in the $Mo(CO)_2(PH_3)_2(NO)H$···HF complex increases by 0.014 Å in $Mo(CO)_2(NH_3)_2(NO)H$···HF, where the H···H interaction strengthens due to the replacement of cis-ligands L (here PH_3) by the stronger σ-donor NH_3. A complementary interaction between F and a H atom of the NH_3 group (the third row of Table 1) in turn increases the H−F lengthening by 0.01 Å. Moreover, some ligands may promote H−R bond splitting, as has been shown for the cationic system $(Cp)Re(NO)(PH_3)H\cdots H_3O^+$.[14] The proton transfer from superacid H_3O^+ to Re, yielding dihydride $(Cp)Re(NO)(PH_3)(H)_2^+(H_2O)$, is accompanied by the recoordination of H_2O from hydride H to the H atom of PH_3 group. With regard to the acidity of HR, the lengthening of the H−O bond in the poor proton donor H_2O in the $Mo(CO)_2(PH_3)_2(NO)H\cdots H-OH$ and half-sandwich $(Cp)Re(NO)(CO)H\cdots H-OH$ is about 0.01 Å, whereas the stronger acid $H-OCF_3$ stretches the H−O bond by about 0.04 Å in the $(Cp)Ru(PH_3)(CO)H\cdots H-OCF_3$ system.

TABLE 1: B3PW91 Calculated[13,14] H···H Bond Lengths $R_{H...H}$ (Å), Stretches ΔR_{H-R} (Å) of H−R Bonds Compared to Free HR, and H-Bond Energies E_{HB} (kcal/mol)

complex	$R_{H...H}$	ΔR_{H-R}	E_{HB}
$Mo(CO)_2(PH_3)_2(NO)(H)\cdots H-F$	1.378	0.040	11.1
$Mo(CO)_2(NH_3)_2(NO)(H)\cdots H-F$	1.300	0.054	15.4
$Mo(CO)_2(NH_3)_2(NO)(H)\cdots H-F$	1.273	0.065	17.1
$Mo(CO)_2(NH_3)_2(NO)(H)\cdots H-OH$	1.647	0.013	13.1
$(Cp)Re(CO)(NO)(H)\cdots H-OH$	1.770	0.006	10.9
$(Cp)Re(CO)(PH_3)(H)\cdots H-OCF_3$	1.458	0.042	9.8

A second important structural feature is the angular component of the H···H bond. This bond is typically quite bent; the angle MHH (Figure 1) is less than 120°. The nature of the potential energy profile[13] allows the R group to approach active centers of coligands L. Besides the coligands, a central metal atom M may promote R−H bond cleavage. Thus, the hydrogen of the HF subunit and Mo atom in the $Mo(CO)_2(NH_3)_2(NO)H$···HF complex approach one another to within 2.8 Å[13] with small but positive Mulliken overlap population of the Mo···HF bonding. Consequently, a weak complementary Mo···HF interaction exists. One may suppose that an agostic interaction contributes to the splitting process.

One may hence consider H−R cleavage as a complicated process: the initial lengthening of the H−R bond upon formation of a H···H bond is promoted to split by complementary interactions with certain coligands and, probably, with the central transition metal atom. The sort of complex which might break the H−R bond of a poor proton donor upon reaction 2 should thus possess a hydride hydrogen of significant proton attracting power, a π-electron-rich transition metal atom (Ru for example), and an arrangement of suitable coligands, such as PH_3 or NH_3, able to recoordinate with the R.

It is the purpose of this study to test these ideas computationally. We have chosen for consideration three chelates of ruthenium, $Ru(H)(H)(PH_2CH_2PH_2)_2$ (**1**), hexacoordinated $Ru(H)(H)(PH_3)_4$ (**2**), and $Ru(H)(H)(NH_3)_4$ (**3**). Both **1** and **2** are models of substituted alkyl and arylphosphine complexes which are used widely as catalysts in homogeneous catalysis. Moreover, HOR additives (for example, H_2O or $HOCH_3$) raise dramatically the catalytic activity of such catalysts.[24] The HF **4**, HCl **5**, H_2O **6**, and $HOCH_3$ **7** molecules were chosen as models of proton donors of various strength and nature of R.

Results and Discussion

The optimized geometries of **1**−**7** along with their atomic charges are reported in Figure 2. The geometries of **1**−**3** make it possible for the H atom of HR to optimally approach the hydride H. It should be noted that **1** is more rigid than **2** and **3**: the PH_2 groups in **1** are fixed firmly whereas the PH_3 (NH_3) groups in **2** and **3** may easily rotate around Ru−P(N) bonds. The N−Ru bonds in **3** are shorter than the P−Ru bonds in **1** and **2** and, consequently, the active hydrogen atoms (H of MH and NH_3) are closer to one another in **3**.

It has been shown[13,14] that the Mulliken procedure is appropriate to consider the trends in the data in a number of MH···HR systems. Therefore, the Mulliken procedure was used for comparison of proton attracting power of hydride H and

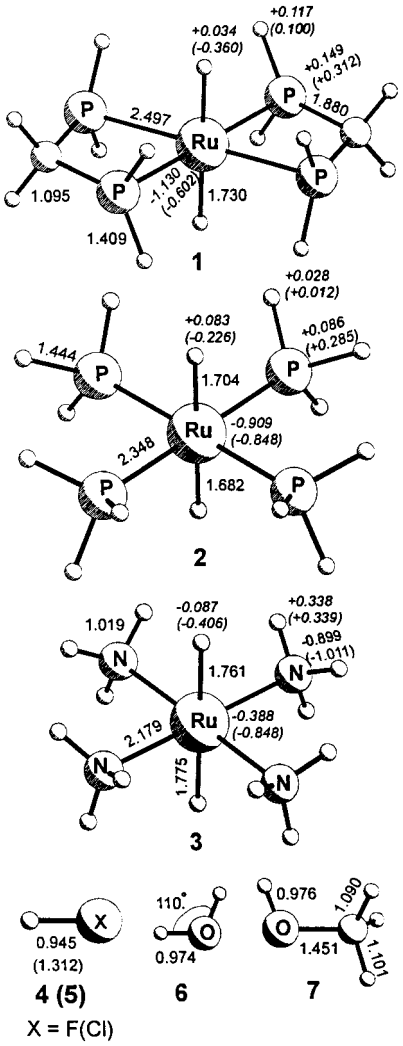

Figure 2. Geometries (in Å and deg) of **1**−**7** and Mulliken(NPA) charges for **1**−**3**.

basicity of metal atoms in **1**−**3**. Since a R···H−P(N) interaction was expected, the electrophilicity of $H_{P,N}$ atoms in **1**−**3** was examined. A comparative analysis of the Mulliken charges shows that hydride H in **1** and **2** are of almost equal proton-attracting power with slight preference for **1**. The hydride H in **3** acquires more electron density as a result of change of PH_3 to stronger σ-donor NH_3. Consequently, the ability of this hydride H to interact with H of the HR grows from **1**(**2**) to **3**. The basicity of Ru increases in the sequence **3**−**2**−**1**. The H_P in **1** are substantially more electropositive than in **2** but significantly less so than H_N in **3**. We thus hypothesize that the ability of $H_{P,N}$ to coordinate with nucleophilic R increases in the sequence **2**−**1**−**3**. The atomic charges have also been calculated using natural population analysis (NPA)[25] to verify the reliability of the Mulliken charges. Although the absolute magnitudes of the NPA charges differ significantly, trends are preserved. (One of the distinct features emerging from NPA analysis is the negative charge of the hydride hydrogens which is significantly undervalued by Mulliken analysis.)

The results of Mulliken and natural population analysis provide an opportunity to define the most important factors that favor H−R splitting. In general, **1** represents the system where all three possible reaction centers are sufficiently active. **2** has two active centers: the hydride H and transition metal; both are less active than in **1**. **3** possesses both the hydride H and the H_N atoms of high activity.

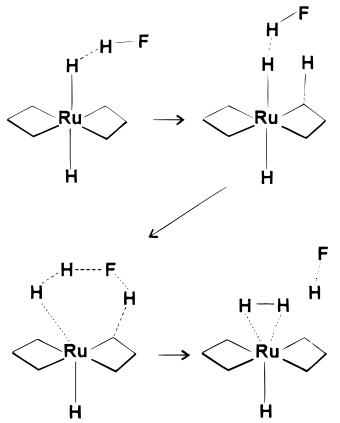

Figure 3. Structural transformations upon reaction of **1** with **4**.

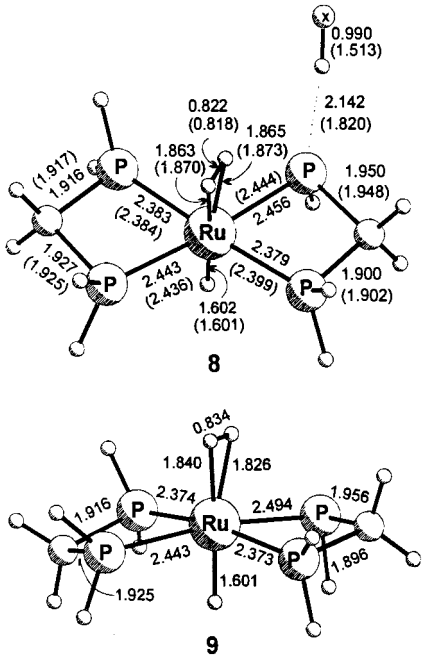

Figure 4. Geometries (in Å) for **8** and **9**. Data in parentheses refer to HCl.

1. H−R Splitting in Ru(H)($PH_2CH_2PH_2$)$_2$(H)···H−R (R = F, Cl, OH, OCH_3). It has been shown[13,14] that the moderate proton donor HF yields MH···HF complexes with some hydrides of transition metals of group VI. Here HF **4** is allowed to interact with trans-dihydride of more basic Ru (VIII) **1** and with hydride H of high proton-attracting power. One might expect the formation of a stable H···H bonded complex with greater lengthening of the H−F bond than in the complexes listed in Table 1. Unexpectedly, two interacting molecules undergo the following transformations illustrated in Figure 3. During geometry optimization of the model structure with initial geometry, corresponding to H···H complex, the H-ligand splits H_{HF} atom from HF yielding a η^2-H_2 molecular complex with H−H distance of 0.822 Å. The fluorine atom, in turn, moves above the RuP_4 plane toward the H atom of one of the PH_2 groups, splits it off, and forms a new HF molecule. The latter HF is coordinated with the P atom, with a P···HF distance of 2.142 Å, yielding complex **8**. Figure 4 illustrates the geometries of the structures described. Although the P···H distance is rather long, the H−F bond in this new HF molecule is stretched by 0.045 Å compared to free HF. The overall energetics of the reaction, computed as the difference between the total energy of **8** and the sum of total energies of subunits **1** and **4**, is 23.8

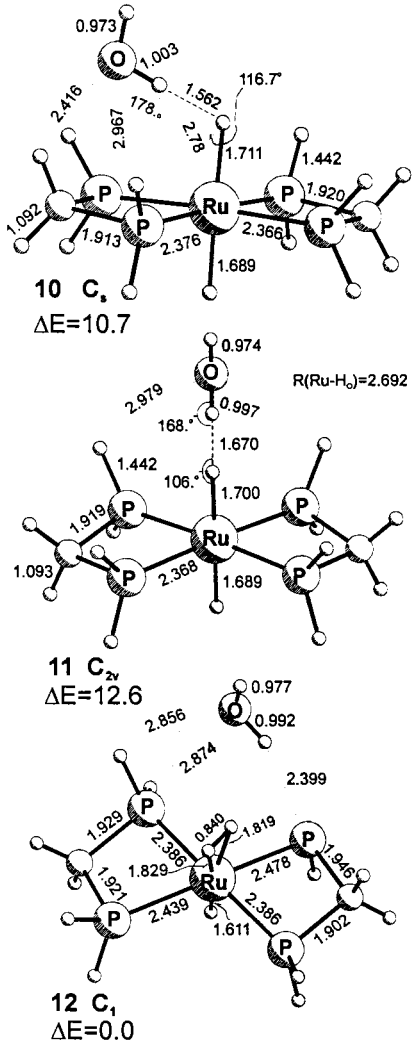

Figure 5. Geometries (in Å and deg) and relative energies (kcal/mol) for **10**−**12**.

kcal/mol (**8** being more stable). No MH···HR or any other intermediates could be identified along this reaction path which advances energetically downhill.

The reaction of the more acidic HCl **5** with **1** proceeds in the same manner as **4**, yielding the similar structure **8**. The energy of reaction is nearly identical to the same quantity for HF. The pertinent geometrical parameters are illustrated in parentheses in Figure 4. As a result of the greater polarizability of HCl compared to HF, the P···H_{Cl} distance is shorter and H−Cl bond longer. Complex **8** may easily release HX, yielding the η^2-H_2 molecular complex **9**.

The related reaction of HF with 16-e hexacoordinated trans-dihydride Mo(H)$(CO)_2(PH_3)_2$(H) was studied in an earlier work.[13] HF does not split upon reaction; a loose intermolecular complex of dihydride type, with a H···H distance of about 1.5 Å and stretched H−F bond of about 1.0 Å, was formed. It was concluded that even in an electronically unsaturated complex, the Mo atom of group VI needs to be rather weakly basic to cleave the H−R bond by agostic bonding. On the other hand, the strong π-acceptor cis-ligand CO reduces the proton-attracting power of hydride hydrogen so that the H···H interaction is too weak for transfer of H_F from F to hydride H.

The next series of computations involve the interaction between the weaker proton donor H_2O and **1**. Unlike HX, water molecule **6** yields H···H bonding complex **10** at the first stage of reaction with **1**, consistent with pathway 2. Figure 5 depicts

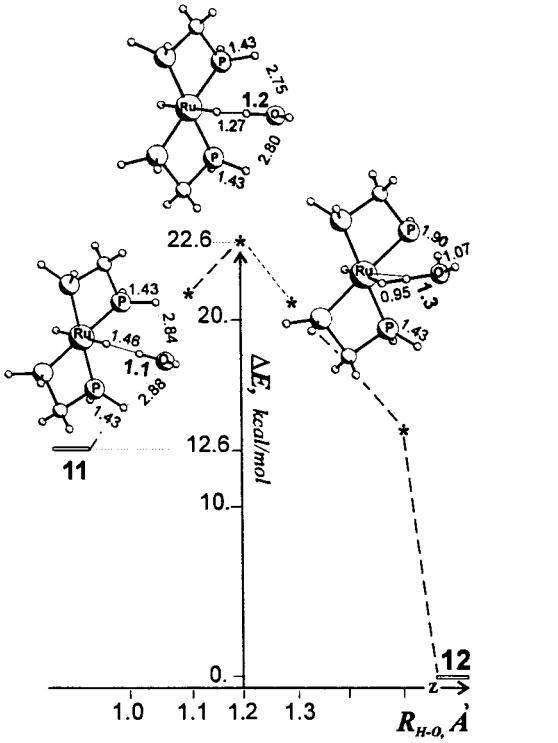

Figure 6. Potential energy profile for **11** → **12** rearrangement. Geometries (in Å) for the steps R_{H-O} = 1.1, 1.2, and 1.3 Å.

the geometries and relative energies of the systems **10**−**12** on the reaction pathway. The H···H complex **10** represents a shallow minimum along the pathway, with lowest normal vibrational frequency 30 cm^{-1}; the complexation energy is 11.8 kcal/mol. DFT frequencies of modes involving the H···H bond lie in the range between 805 and 760 cm^{-1}, in agreement with HF/3-21G results[13] for the related Mo$(NO)(CO)_2(PH_3)$H···HF complex (969−775 cm^{-1}). The H−O bond stretches by 0.029 Å compared to free H_2O. The oxygen atom of the H_2O in **10** is coordinated with H atoms of the CH_2 and PH_2 groups, imparting C_s symmetry to the complex. These weak O···H interactions are likely electrostatic since the pertinent distances are rather long and the P−H and C−H bonds involved in interaction are not stretched. The next possible sites for oxygen coordination are the H atoms of PH_2 groups which belong to different rings of the chelate. Indeed, C_{2v} isomer **11** was found, 1.9 kcal/mol less stable than **10**. The η^2-H_2 structure **12**, formed by analogy with **8,** is 10.7 kcal/mol more stable than **10** (the pertinent experimental value[11] for related systems is 17 ± 3 kcal/mol). Like **8**, the complexation energy of **12** is quite attractive, 26.6 kcal/mol, partly due to additional coordination of the water oxygen atom with the H atoms of neighboring PH_2 group.

The barrier for the H···H → η^2-H_2 rearrangement was estimated by stepping along the reaction coordinate from **11** to **12**. The H−O distance was chosen as the reaction coordinate and was increased in steps of 0.1 Å. All other geometric parameters were optimized at each step. Attempts to reach **12** from minimum **10** were unsuccessful: instead, **10** was transformed directly into **11**. Consistent with symmetry, one may suppose that four shallow minima exist with respect to rapid rotation of the ROH···H fragment around the pertinent Ru−H bond.

Figure 6 illustrates the potential energy profile of the **11** → **12** conversion, along with geometries corresponding to the H−O distances R_{H-O} of 1.1, 1.2, and 1.3 Å. An initial lengthening of the H−O bond in the range between 1 and 1.2 Å is accompanied

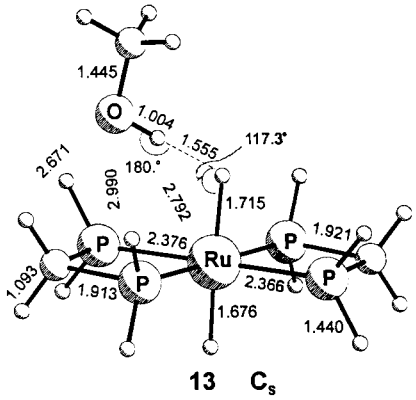

Figure 7. Geometry (in Å and deg) for **13**.

by shortening of the H···H bond and by weakening of one of the additional O···H(P) interactions, relative to the other. The stretch of the H−O bond to 1.3 Å promotes the transfer of the H atom from O to hydride H and causes the transfer of a H atom from PH_2 to the oxygen of the OH fragment. The H_2-molecular ligand and new water molecule form; the potential energy drops, and the entire system relaxes to complex **12**. The computed barrier of 10.0 kcal/mol for this process is in good agreement with dynamic NMR data.[11]

The interaction of **1** with the still more acidic $HOCH_3$ yields H···H complex **13** depicted in Figure 7. The complexation energy is 10.3 kcal/mol. The geometry and energetics of **13** are very close to the related complex **10**. It is suggested that pathway 2 should be similar for both H_2O and $HOCH_3$ by analogy with HF and HCl.

In summary, **1** and HR yield upon reaction 2 a multi-H-bonded Ru−H···H−R···H−P system, containing both H···H and conventional H bonds. H−R cleavage occurs via concerted (not fully synchronous) transfer of two hydrogen atoms from R to hydride H, and from P to R, over a small barrier of 10 kcal/mol for H_2O and without a barrier for HX. A similar mechanism was suggested for the cleavage of H−O bonds in water by Lee et al.[26,27] It has been shown for the neutral H-bonded clusters of H_2O and for related water clusters including HF, HCl, and H_2S that the H−O bond cleaves upon concerted transfer of two H atoms, almost without barrier.

2. H−R Cleavage in $RuH(PH_3)_4H\cdots H-R$ (R = F, OH). Compared to **1**, dihydride **2** possesses less active H(P) and Ru atoms. Computed results show that H−R cleavage is inhibited in **2**. The geometries of calculated structures formed by interaction of **2** with **4** and **6** are illustrated in Figure 8. Dihydride **2** yields the H···H complexes **14** and **15** with **4** and **6,** respectively. Reaction energies are 17.8 and 15.9 kcal/mol, respectively. The η^2-H_2 complexes **16** and **17** are more stable than corresponding H···H complexes, but by only 4.9 and 7.0 kcal/mol. Unlike **12**, there is no additional interaction between R and H atoms of neighboring PH_3 group found in **17**.

To estimate the barriers of the H···H → η^2-H_2 rearrangements **14** → **16** and **15** → **17,** the H−R distances were chosen as reaction coordinates. Distinct from **1**, the H atoms of PH_3 acquire very small positive charge in **2**. Therefore, the interaction with nucleophilic R and, consequently, the formation of a multi-H-bonded complex, are questionable. Indeed, attempts to reach **16** (**17**) from **14** (**15**) by moving along this reaction coordinate were unsuccessful. Neither the F nor the OH fragments form a chemical bond with H_P. Instead, a very weak multicoordinated electrostatic interaction of R with a number of H_P and P atoms was observed. Both potential energy profiles, along with pertinent geometries corresponding to H−R length of 1.7 Å, are depicted in Figure 9. The potential energy increases by about 30 kcal/mol in the case of HOH and by some 12 kcal/mol for HF, at an H−R distance of about 1.7 Å. These values barely change as one progresses further along the reaction coordinate. The PH_3 groups rotate easily around Ru−P bonds, synchronously with motion of the R fragment, providing multicoordinated electrostatic interactions at each step. No intermediates were noted.

This type of reaction coordinate yields only a crude assessment of barriers and is too approximate to fully study the reaction mechanism for a complicated PES. Nevertheless, the differences between calculated results for **1** and **2** highlight certain trends. The high proton-attracting power of hydride hydrogen is necessary but not sufficient to attain low barrier cleavage of the H−R bond. In the case when the M−H···H−R···H−L complex cannot be easily formed due to low activity of H_L, a mechanism with a low barrier for H−R splitting is improbable. Indeed, experiment[12] yields a high barrier for (2) in the case of (Cp)Ru(CO)(NO)H···H−OR and (Cp)Re(PH_3)(NO)H···H−OR; a multi-H-bonded complex does not form at all in the former complex and is questionable in the latter. The R group may form donor−acceptor bonds with atoms other than hydrogen, as for example with P atoms as in the case of **2**. Mechanisms of H−R bond cleavage in such donor−acceptor-bonded complexes may warrant further investigations.

3. H−R Splitting in $RuH(NH_3)_4H\cdots H-R$ (R = F, OH). The model dihydride **3** represents a structure with the highest proton attracting power of its hydride H and the most electropositive H_N. Moreover, these atoms are relatively close to one another. These particular features should define the pathway (2) and the structure of the η^2-H_2 product. One can expect that hydride H in **3** ought to form the strongest H···H bond.

The computed results show that interaction between **3** and HF proceeds almost as in the case of **1** depicted in Figure 3, without barrier or intermediates, exothermic by 50.7 kcal/mol. H−F cleavage occurs via transfer of the H_{HF} atom from F to hydride hydrogen; the η^2-H_2 molecular ligand forms with H−H distance of 0.817 Å. The subsequent part of the pathway mirrors the peculiarities of **3**. The fluorine atom moves above the RuN_4 plane toward the H_N atoms which belong to the neighboring NH_3 groups, forming a H_N−F−H_N bridge. The η^2-H_2 complex **18**, with bridged F atom, is illustrated in Figure 10. Distinct from the P atom in **1**, the more electronegative N in **3** does not lose its H atom upon interaction with F. The N−H bond lengths of bridged H atoms stretch by some 0.07 Å. A structure of **8** type, with a weakly coordinated HF molecule, was not found for **3**.

The peculiarities of **3** are displayed more clearly upon reaction with H_2O. Similar to **1, 3** yields the H···H complex labeled **19** in Figure 10. The H−O bond in **19** is stretched by 0.103 Å, more than in **12** and **17** and in the systems listed in Table 1. The additional O···$(H(N))_2$ bonds in **19** are stronger than in the related complex **12**: the O···H lengths are rather short and pertinent H−N bonds involved in interaction are stretched by 0.01 Å compared to "free" H−N bonds. These results suggest a low barrier for the H−O cleavage in **3**. The complexation energy of **19** is 32.5 kcal/mol.

In summary, energetically facile H−R cleavage may occur via the mechanism of transfer of H_R from R to hydride hydrogen, with later bonding of R to ligands. No influence of the smaller basicity of Ru is noted.

Conclusions

The 18-e transition metal hydrides may split H−R covalent bonds through H···H bonding, yielding a η^2-H_2 complex upon

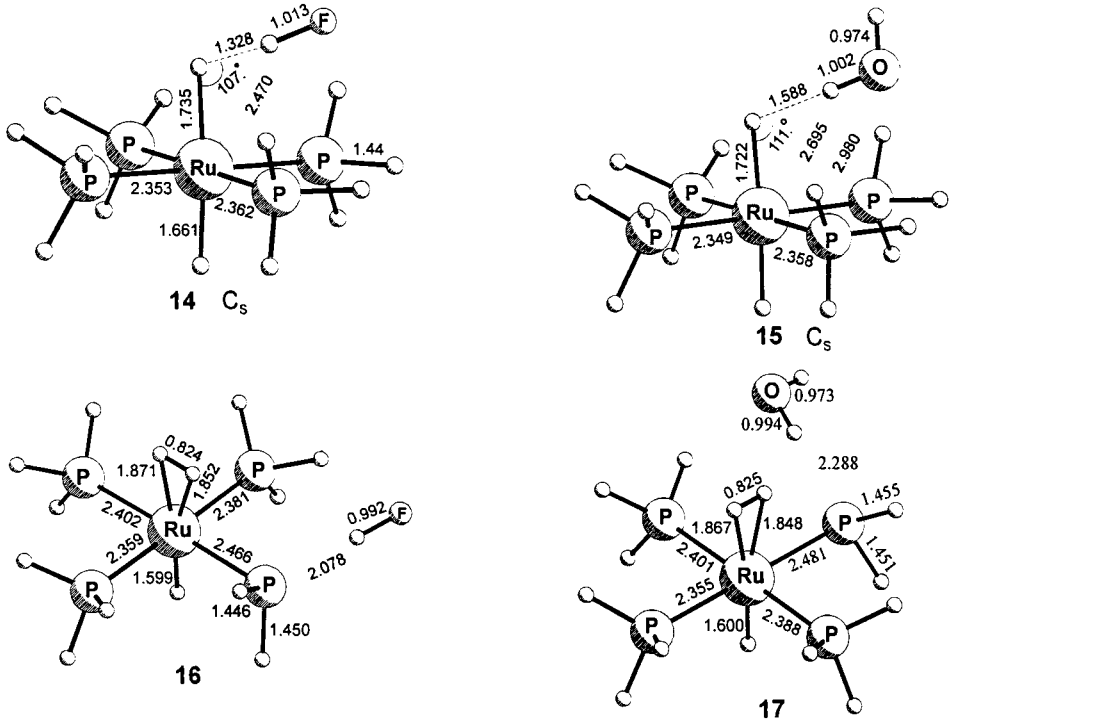

Figure 8. Geometries (in Å and deg) for**14**−**17**.

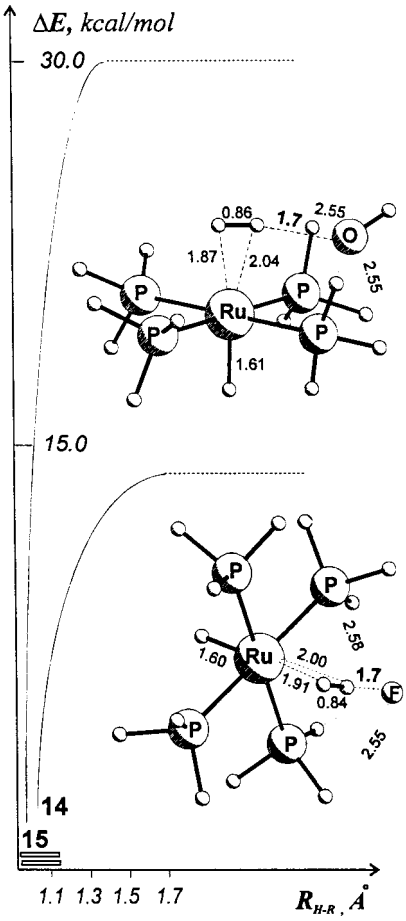

Figure 9. Potential energy profiles for the lengthening of H−R bonds in **14** and **15**. Geometries (in Å) for the step $R_{H-R} = 1.7$ Å.

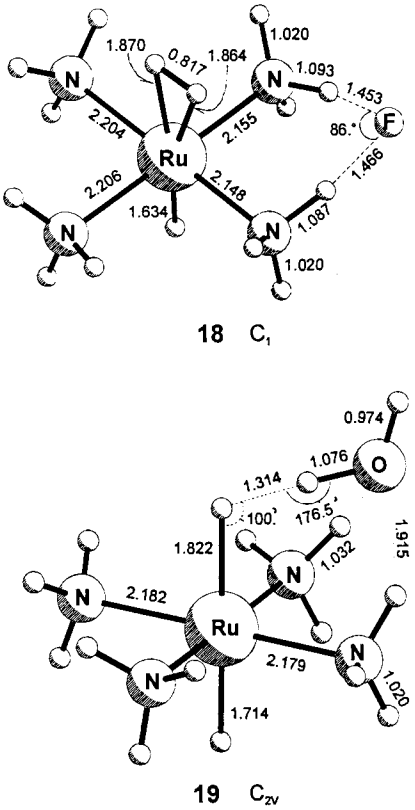

Figure 10. Geometries (in Å and deg) for **18** and **19**.

reaction with poor and moderate proton donors. The reaction proceeds exothermically over a small barrier for the poor H-donors H−OR, or without a barrier for the stronger H donors HX. The MH is best equipped for this reaction with a hydride hydrogen of high proton-attracting power and a suitable arrangement of ligands able to bond with the R group of HR. As opposed to 16-e complexes, the basicity of the transition metal is not a major factor in H−R cleavage. Two similar but distinct low-barrier mechanisms were identified; the more favorable pathway depends on the nature of the ligands. The H−R bond may cleave, involving transfer of H_R from R to hydride H, while the H_L atom transfers from ligand to R, forming a multi-H-bonded M−H···H−R···H−L system. A η^2-

H_2 complex is the result, along with a weakly coordinated HR. Along the second pathway, the transfer of H_R to hydride H in the multi-H-bonded system is accompanied by bonding of R to the ligands. Higher barriers are expected for H−R splitting in systems where the formation of a multi-H-bonded complex is not possible or difficult. Although the influence of solvent was excluded from consideration, it may be supposed that solvent involvement with the multi-H-bonded system may significantly reduce the barrier of rearrangement.

Acknowledgment. G.O. thanks the Ministry of General and Professional Education of Russian Federation (grant N97-9.1-288) for support of this research.

References and Notes

(1) *Transition Metal Hydrides;* Dedieu, A., Ed.; VCH: New York, 1992.

(2) Heinekey, D. M.; Oldham, W. J. *Chem. Rev.* **1993**, *93*, 913.

(3) Shubina, E. S.; Belkova, N. V.; Epstein, L. M. *J. Organomet. Chem.* **1997**, *536*−*537*, 17.

(4) Controy-Lewis, F. M.; Simpson, S. J. *J. Chem. Soc., Chem. Commun.* **1987**, 1675.

(5) Chinn, M. S.; Heinekey, D. M.; Payne, N. G.; Sofied, C. D. *Organometallics* **1989**, *8*, 1824.

(6) Chinn, M. S.; Heinekey, D. M. *J. Am. Chem. Soc.* **1990**, *112*, 5166.

(7) Li, Z.; Taube, H. *Science* **1992**, *256*, 210.

(8) Wessel, J.; Lee, J. C.; Peris, E.,; Yap, G. P. A.; Fortin, J. B.; Ricci, J. S.; Sini, G.; Albinati, A.; Koetzle, T. F.; Eisenstein, O.; Rheingold, A. L.; Crabtree, R. A. *Angew. Chem., Int. Ed. Engl.* **1995**, *34*, 2507.

(9) Shubina, E. S.; Belkova, N. V.; Krylov, A. N.; Vorontsov, E. V.; Epstein, L. M.; Gusev, D. G.; Neidermann, M.; Berke, H. *J. Am. Chem. Soc.* **1996**, *118*, 1105.

(10) Belkova, N. V.; Shubina, E. S.; Ionidis, A. V.; Epstein, L. M.; Jacobsen, H.; Messmer, A.; Berke, H. *Inorg. Chem.* **1997**, *36*, 1522.

(11) Ayllon, J. A.; Gervaux, C.; Sabo-Etienne, S.; Chaudert, B. *Organometallics* **1997**, *16*, 2000.

(12) Epstein, L. M.; Shubina, E. S. *Proton Transfer and Hydrogen Bonding with Transition Metal Atoms and Hydride Hydrogen by IR and NMR Studies.* Presented at Hydrogen Transfer: Experiment and Theory, International Discussion Meeting, Berlin, September 10−13, 1997.

(13) Orlova, G.; Scheiner, S. *J. Phys. Chem. A* **1998**, *102*, 260.

(14) Orlova, G., Scheiner, S. *J. Phys. Chem. A* **1998**, *102*, 4813.

(15) Parr, R. G.; Yang, W. *Density-Functional Theory of Atoms and Molecules*; Oxford University, New York, 1989. *Density Functional Methods in Chemistry*; Labanowski, J. K., Andzelm, J. Eds.; Springer-Verlag: New York, 1991.

(16) Becke, A. D. J. Chem. Phys. **1993**, *98*, 5648. Perdew, J. P.; Wang, Y. *Phys. Rev. B* **1992**, *45*, 13244.

(17) Frisch, M. J.; Trucks, G. W.; Schlegel, H. B.; Gill, P. M. W.; Johnson, B. G.; Robb, M. A.; Cheeseman, J. R.; Keith, T.; Petersson, G.; Montgomery, J. A.; Raghavachari, K.; Al-Laham, M. A.; Zakrzewski, V.; Ortiz, J. V.; Foresman, J. B.; Peng, C. Y.; Ayala, P. Y.; Chen, W.; Wong, M. W.; Andres, J. L.; Replogle, E. S.; Gomperts, R.; Martin, R.; Fox, D. J.; Binkley, J. S.; Defrees, D. J.; Baker, J.; Stewart, J. P.; Head-Gordon, M.; Gonzalez, C.; Pople, J. A Gaussian, Inc., Pittsburgh, PA, 1995.

(18) Hay, P. J.; Wadt, W. R. *J. Chem. Phys.* **1985**, *82*, 270, 299.

(19) Wadt, W. R.; Hay, P. J. *J. Chem. Phys.* **1985**, *82*, 284. Dunning, T. H.; Hay, P. J. In *Modern Theoretical Chemistry*; Schaefer, III, H. F., Ed.; Plenum: New York, 1976; pp 1−28.

(20) (a) Ziegler, T.; Fan, L. *J. Chem. Phys.* **1991**, *95*, 7401. (b) Delly, B.; Wrinn, M.; Luthi, H. P. *J. Chem. Phys.* **1994**, *100*, 5785.

(21) (a) Becke, A. D. *Phys. Rev. A* **1988**, *38*, 3098. (b) Lee, C.; Yang, W.; Parr, R. G. *Phys. Rev. B* **1988**, *37*, 785. Miechlish, B.; Savin, A.; Stoll, H.; Preuss, H. *Chem. Phys. Lett.* **1989**, *157*, 200.

(22) Jonas, V.; Thiel, W. J. *Chem. Phys.* **1996**, *105*, 3636; **1995**, *102*, 8474. Bytheway, I.; Bacskay, G. B.; Hush, N. S. *J. Phys. Chem.* **1996**, *100*, 6023. Bytheway, I.; Bacskay, G. B.; Hush, N. S. *J. Phys. Chem.* **1996**, *100*, 14899.

(23) Lohrenz, J. C. W.; Woo, T. K.; Fan, L.; Ziegler, T. *J. Organomet. Chem.* **1995**, *497*, 91. Lohrenz, J. C. W.; Woo, T. K.; Ziegler, T. *J. Am. Chem. Soc.* **1995**, *117*, 12793. Margl, P.; Deng, L.; Ziegler, T. *J. Am. Chem. Soc.* **1998**, *120*, 5517.

(24) Jessop, P. G.; Hsiao, Yi; Ikariya, T.; Noyori, R. *J. Am. Chem. Soc.* **1996**, *118*, 344.

(25) Reed, A. E.; Weinstock, R. B.; Weinhold, F. *J. Chem. Phys.* **1988**, *83*, 735.

(26) Torser, D. J.; Lee, C.; Fitzgerald, G. *J. Chem. Phys.* **1996**, *104*, 5555.

(27) Lee, C.; Sosa, C.; Planas, M. *J. Chem. Phys.* **1996**, *104*, 7081.